# Thermal and Photo Dual-Responsive Core-Shell Polymeric Nanocarriers with Encapsulation of Upconversion Nanoparticles for Controlled Anticancer Drug Release

Xiaotao Wang[a]*, Chuang Liu[a], Zhenhua Li[a], Chak-Yin Tang[b]*, Wing-Cheung Law[b]*, Xinghou Gong[a], Zuifang Liu[a], Yonggui Liao[c], Gaowen Zhang[a], Shijun Long[a], Ling Chen[b]

a. Hubei Provincial Key Laboratory of Green Materials for Light Industry, Collaborative Innovation Center for Green Light-weight Materials and Processing, School of Materials Science and Engineering, Hubei University of Technology, Wuhan, Hubei Province 430068, P.R. China.

[b] Department of Industrial and Systems Engineering, The Hong Kong Polytechnic University, Hung Hom, Kowloon, Hong Kong SAR, P.R. China

[c] Key Laboratory for Large-Format Battery Materials and System, Ministry of Education, School of Chemistry and Chemical Engineering, Huazhong University of Science and Technology, Wuhan 430074, China

*Corresponding authors:

cy.tang@polyu.edu.hk, roy.law@polyu.edu.hk, xiaotaowang@hbut.edu.cn

## Abstract

A thermal and photo dual-responsive drug delivery system is newly designed for controlled anticancer drug delivery. The concept of this design is to encapsulate upconversion nanoparticles in a photoresponsive polymer to produce core-shell nanoparticles, in which NIR light is converted to UV/visible light to isomerize crosslinked bis(methacryloylamino)-azobenzene for the control of drug release. A facile scheme, which gives the details of two-step solvothermal treatment, microemulsion, distillation precipitation polymerization, and drug loading, is proposed to realize the design. The dual-responsive drug release behaviors of the system are reported to provide the

information for potential development of cancer therapy. It is also found that the Baker−Lonsdale model is suitable for describing the drug release kinetics of this system and the values of the diffusion coefficient under various conditions are determined experimentally.

## 1. Introduction

In recent years, stimuli-responsive nanoparticles, that can deliver and release the therapeutic payloads in a controlled manner, have played increasingly important roles in designing nanocarriers for anticancer drug delivery. The nanocarriers were usually fabricated by assembling stimuli-responsive polymers, that exhibit physical changes upon an exposure of external stimuli, such as pH, electricity, light, enzyme and temperature [1-5]. Due to the unique features of inorganic nanomaterials[6-9], such as high luminescence, photothermal generation, plasmonic behavior and upconversion optical properties, an incorporation of inorganic nanostructures with stimuli-responsive polymers has become a powerful technique to enhance the nanocarriers performances. To this end, many strategies have been developed. Light responsive nanoparticles, that were fabricated from azobenzene [10-11], o-nitrobenzyl, dithienylethenes [12-13], spiropyran [14], and coumarin [15], were typically found as these exogenetic triggered nanoparticles have flexible spatial and time freedom for controlling the release of payloads at a specific time and location with relatively high precision. Self-assemble of block copolymer was one of the methods to prepare light responsive micelles or nanoparticles. In this case, most of the photoisomeric moieties are UV-responsive, thus payloads were mainly released by an UV irradiation [16]. For biological applications, however, two challenges are remained. Due to its high energy and high absorption by the biological tissues (i) UV is usually harmful to the biological bodies and difficult to penetrate to the deep tissue; (ii) self-assemble micelles may not be stable enough in biological environment and burst release may occur after the dissociation under light.

For biomedical applications, especially when the drug dosage is required to be critically controlled (e.g. anticancer drugs and diamondoid derivatives for Alzheimer's disease), remotely trigger drug release using longer-wavelength (e.g. NIR) light source is more suitable. Upconversion

nanomaterials are of particular interest because they absorb multiple photons of lower energy (small bandgap energy) and transmit to larger bandgap emission (i.e. UV or visible range). Recently, upconversion nanoparticles encapsulated in light responsive micelles have been widely studied. Zhao and co-workers firstly dissociated upconversion nanoparticles packed block copolymer micelles [17]. Chen et al. synthesized amphiphilic spiropyran/(N-isopropylacrylamide) block copolymer and self-assemble with upconversion nanoparticles [18]. After NIR irradiation, the composite successfully disassembled to realize controlled release. Wu and coworkers also constructed NIR responsive nanomicelles through amphiphilic copolymer containing azobenzene through self-assembly method [19]. The self-assemble method was utilized to composite upconversion nanoparticles and photoresponsive micelles which realize NIR responsive release and more suitable for bio-systems. However, challenges for self-assemble polymer nanoparticles, such as structure stability and burst release, are still exist in the bio-system [20-21].

In our previous study, we focused on the issue of controlled drug loading and release by using a distillation precipitation polymerization process, in which silica was used as a reaction template (eventually dissolved) and bis(mathacrylolamino) azobenzene was used as the crosslinker [22]. Distillation precipitation polymerization was chosen because relative stable polyazobenzene nanospheres can be synthesized, whereas the photoresponsive micelles prepared from block copolymer were not very stable due to the large steric resistance of azobenzene. Our distillation precipitation polymerization begins with lower concentration of monomer, which can effectively reduce the aggregation of particles. By distilling solvent at a constant speed, a high monomer conversion could be achieved and it is the precondition of forming polyazobenzen particles. We found that the permeability of these nanocapsules can be adjusted by UV irradiation and both the controlled encapsulation and release of molecules were successfully demonstrated. In current work,

efforts are devoted to improve the stability of nanoparticles and study the potential for biomedical applications. In this paper, a new design of a robust and multiple responsive drug delivery polymeric system based on incorporating photo- and thermal-responsives polymers with UCNPs is presented. UCNP-PNIPAM core-shell nanoparticles are formed by using a modified distillation precipitation polymerization process [23-25]. Monodispersed UCNP core transforms the NIR light to UV/visible light to isomerize crosslinked BMAAB that can produce the photomechanical effect within the shell and alter the controlled release behaviors. The NIR and thermo- responsive controlled release behaviors have also been studied and explored, with the aim to achieve exogenetic (NIR light) and endogenous (temperature) control in one system. With this unique feature, i.e. thermo- and NIR responsive, the prepare nanoparticles can act as potential drug carriers for targeted cancer therapy.

## 2. Experimental Section

### *2.1 Materials*

Yuelong New Material Co., Shanghai, China supplied rare earth oxides ($Y_2O_3$, $Yb_2O_3$, $Tm_2O_3$). Oleic acid (OA; 90%), 1-octadecene (ODE; 95%), N-Isopropylacrylamide (NIPAM) and Divinylbenzene (DVB) were purchased from Aladdin reagent Co., Ltd, Shanghai, China. Sodium hydroxide, ammonium fluoride, hydrochloric acid (HCl; 36.7%), ethanol, chloroform, cyclohexane, ammonia aqueous solution (33 wt%), tetraethyl orthosilicate (TEOS), methacrylic acid were supplied by Sinopharm Group Chemical Reagent Co., Ltd, Shanghai, China. Igepal CO-520 was purchased from Sigma-Aldrich Trading Co., Ltd, Shanghai, China. 3-Methacryloxypropyltrimethoxysilane (MPS) was obtained from Organic Silicon Company at Wuhan University, China. High-purity azobis (isobutyronitrile) from Huacheng Industrial Co., Ltd, Shanghai, China was recrystallized by ethanol.

*2.2 Synthesis of oleic acid (OA) coated $NaYF_4$: $Yb^{3+}/Tm^{3+}$ nanoparticles (OA-$NaYF_4$: Yb/Tm)*

The synthesis of OA-$NaYF_4$: Yb, Tm nanoparticles can be realized by using the solvothermal procedure based on the previously reported method. In a typical experiment, 0.795 mmol of $YCl_3$, 0.200 mmol of $YbCl_3$ and 5 μmol of $TmCl_3$ were dissolved in water and added into a 100 mL three-necked round-bottom flask containing 7 mL of oleic acid and 15 mL of 1-octadecene mixture respectively. To get rid of water and oxygen, the mixture was slowly heated to 120 °C under $N_2$ flow. Then the mixture was slowly heated to 160 °C and maintained for 40 min to form a clear light yellow solution. After cooling down to room temperature by removing the heating mantle while stirring, 5 mL of NaOH-methanol stock solution and 8 mL of $NH_4F$-methanol stock solution were added into a 15 mL centrifuge tube. The tube was sealed and the solution was mixed for 10 s. Then the mixture was quickly added into the reaction flask. The solution was vigorously stirred at room temperature for 1 h. After the evaporation of methanol, the solution was heated to 300 °C under $N_2$ and kept at this temperature for 90 min. The collection of OA-$NaYF_4$: Yb, Tm nanoparticles was carried out by centrifugation at 8000 rpm for 40 min. Then OA-$NaYF_4$: Yb, Tm nanoparticles were washed with ethanol/chloroform three times prior to use.

*2.3 Synthesis of OA-$NaYF_4$: Yb/Tm@$NaYF_4$ (UCNPs) core-shell nanoparticles*

The $NaYF_4$: Yb, Tm@$NaYF_4$ core-shell nanoparticles were synthesized using about 1 mmol of OA-$NaYF_4$: Yb, Tm nanoparticles prepared using the same method as described above. Typically, a solution of $YCl_3$ (1 mmol) was added into 7 mL of oleic acid and 15 mL of 1-octadencene mixture in a 100 mL flask. To get rid of water and oxygen, the mixture was slowly heated to 120 °C under $N_2$ flow. Then the mixture was slowly heated to 160 °C under $N_2$ flow and maintained for 40 min to form a clear light yellow solution. Until it is cooled down to room temperature, approximately 9 mL oleic acid (OA) coated $NaYF_4$: $Yb^{3+}/Tm^{3+}$ nanoparticles were added into a 15 mL centrifuge

tube. Then the solution was stirred at room temperature for 30 minutes. To remove chloroform in a stream of nitrogen, the mixture was slowly heated to 86 °C. After cooling down to room temperature by removing the heating mantle while stirring, 5 mL of NaOH-methanol stock solution and 8 mL of $NH_4F$-methanol stock solution was added into a 15 mL centrifuge tube. The tube was sealed and the solution was mixed for 10 s. Then the mixture was quickly added into the reaction flask. The solution was vigorously stirred at room temperature for 1 h. After the evaporation of methanol, the solution was heated to 300 °C under $N_2$ and kept at this temperature for 90 min before it was allowed to cool naturally to room temperature. The same washing procedure was followed as mentioned above and sample was re-dispersed in 10 mL cyclohexane.

*2.4 Coating of silica on the UCNPs (UCNPs@$SiO_2$)*

Oleic acid-coated UCNPs can only disperse well in nonpolar solvents. To prepare water soluble UCNPs, reverse microemulsion approach was used to modify the surface of nanoparticles. A $SiO_2$ shell was applied as follows: Specifically, 1.3 mL of Igepal CO-520, 20 mL of cyclohexane and 0.7 mL of UCNPs in cyclohexane was added in a 100 mL flask under magnetic stirring for 10 minutes. Next, 160 uL of ammonia aqueous solution (33 wt%) was introduced to the microemulsion system and sonicated for 30 min to form a transparent reverse microemulsion. Then, 250 uL of TEOS was added, and the silica coating reaction was completed after 24 h. Lastly, about 2.5 mL of MPS was added, and the reaction was continued for another 24 h. Ethanol was used to wash the UCNPs@$SiO_2$ when they were precipitated by acetone. Then UCNPs@$SiO_2$ nanoparticles were washed with ethanol three times.

*2.5 Synthesis of bis(methacryloylamino)-azobenzene (BMAAB)*

4,4'-diaminoazobenzene (DAAB) was synthesized according to the references [22]. BMAAB was prepared using a temperature dehydration reaction. In a typical experiment, 2 g of DAAB was dissolved in 800 mL of chloroform. A solution of methacrylic acid (10 mL) and EDC·HCl (3.6 g) were added into the flask. The reaction was maintained at room temperature for three days. The organic solution was washed twice with water, dried with magnesium sulfate, and evaporated under reduced pressure. Ethanol was used to purify the crude product. The crude product was dried at 50 °C.

*2.6 Synthesis of PNIPAM coated UCNPs@$SiO_2$ (i.e. Dual-responsive nanocarriers, DR-NCs)*

The PNIPAM coated UCNPs@$SiO_2$ microspheres have been accomplished using distillation precipitation polymerization. Typically, 30 mg of UCNPs@$SiO_2$ was uniformly dispersed into 70 mL of acetonitrile by ultrasonication about 30 min in flask. Then, adding crosslinking agent BMAAB (85 mg), thermosensitive monomer NIPAM (213 mg), co-crosslinker DVB (40 μL) and initiating agent AIBN (5.06 mg, 3 wt% of total monomer) into the round-bottom flask in order. This setup consists of a four-neck, 100-mL round-bottom flask equipped with an oil-water separator, a condenser, a stir bar, a thermometer, a receiver and nitrogen protection device. To get rid of the air in the reactor, replaced nitrogen about three times and then connected the gas to the condenser. The solution was heated from room temperature to 80 °C within 30 min and kept for 15 min, then raise the temperature to 100 °C. After distilling about half of the acetonitrile within 3.5 h (including heating time), a small amount of inhibitor was added to terminate the reaction. DR-NCs were obtained by centrifuging the reaction mixture at 12,000 rpm for 50 min at room temperature and the nanoparticles were washed with ethanol for several times until the supernatant fluid became colorless.

*2.7 Loading of Doxorubicin hydrochloride (DXR)*

A mixture of 20 mL of DXR solution (0.6 mg/mL) in deionized water and DR-NCs (60 mg) were magnetically stirred for 24 hours at ambient temperature. After centrifugation of the resulting solution at a speed of 14000 rpm, the resultant precipitation was washed with ethanol. The whole washing process was completed in 15 min. The loading capacity of the DXR molecules was measured using UV-Vis absorption spectroscopy at a wavelength of 480 nm. The DXR-loaded DR-NCs (DXR-DR-NCs) were dried as powders.

*2.8 Thermal-controlled release behavior of the DXR-DR-NCs*

A total of 10 mg of DXR-DR-NCs were added to 5 mL of water and contained in a dialysis bag having 8,000-14,000 kDa molecule-weight cut-off. The dialysis bag was placed in a container with 13 mL of water and maintained at 25 °C in a water bath. Periodically, about 4 mL of the solution was withdrawn from the container for absorbance analysis to access the concentration of DXR discharged in the solution. The analysis was conducted at an excitation wavelength of 480 nm before the test solution was returned to its container.

*2.9 Photo-controlled release behavior of the DXR-DR-NCs*

The procedure follows that described in the above steps. In addition, two more samples were prepared. Each of these three containers was irradiated with NIR, visible light irradiation. Periodically, about 4 mL of solution was withdrawn from the container for fluorescent spectroscopic analysis to access the concentration of DXR discharged in the solution. The analysis was conducted at an excitation wavelength of 480 nm before the test solution was returned to its container.

*2.10 Characterizations*

A Bruker Equinox 55 Fourier spectrometer was utilized to record Fourier transform infrared (FTIR) spectra using a KBr disc. Transmission electron microscopy (TEM) was performed on a Tecnai G 220 electron microscope (PEI Co.) at 200 kV. The water contact angles of DR-NCs nanoparticles were observed through the contact angle measuring instrument JC2000D Shanghai Zhongchen Digital Technology Equipment Co., Ltd. A Hitachi F-500 fluorescence spectrophotometer equipped with a 980 nm near-infrared light source (2.5W) was utilized to record the emission of UCNPs spectra.

## 3. **Results and Discussion**

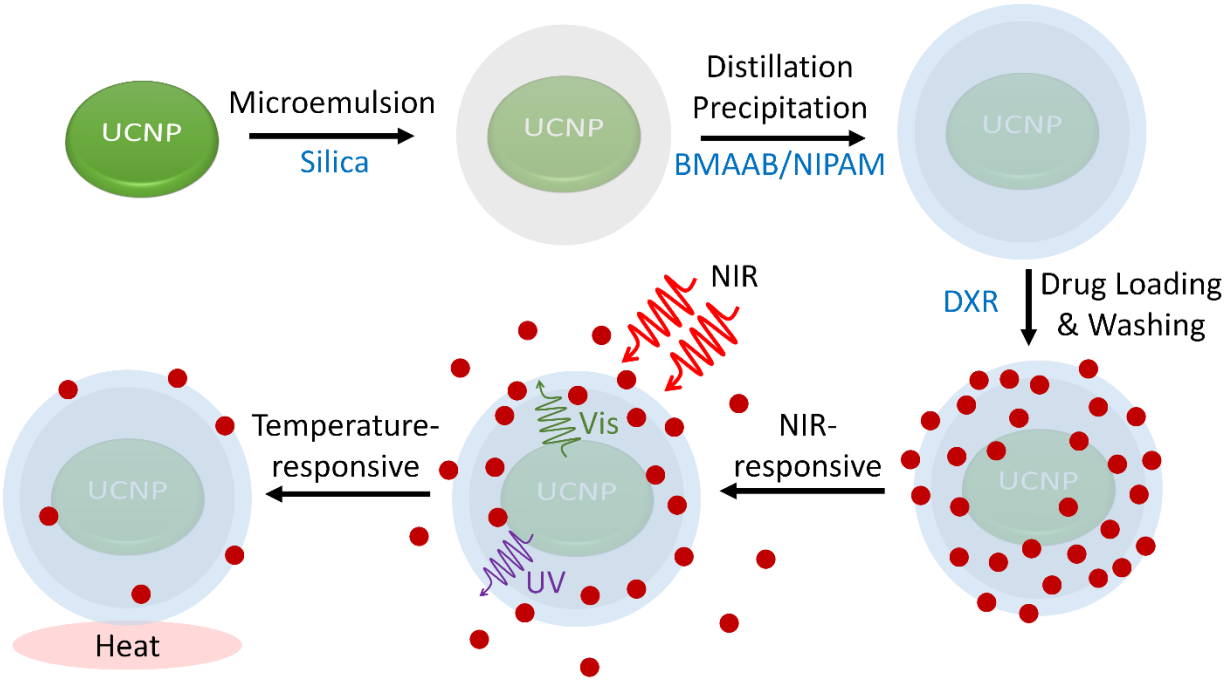


Scheme 1. Synthetic route of DR-NCs and the loading and release of DXR

**Scheme 1** illustrates the synthetic route of the DR-NCs and the procedures for loading and controlled release of DXR. **Figure 1a** shows monodispersed OA-NaYF4: Yb/Tm nanoparticles (core) and the average diameter is about 22 nm. The successful formation of uniform core-shell UCNPs can be clearly observed in **Figure 1b**. The average size of the "rod-shape" UCNPs was

increased to 40 nm × 24 nm after the deposition of the $NaYF_4$ shell. The as-prepared UCNPs were passivated with thin layer of oleic acid molecules, as shown in the FTIR spectra (**Figure S1**). The layer of oleic acid molecules can keep them from aggregating and facilitate a dispersion in non-polar solvents.

Silica was chosen as an intermediate layer which could be further modified with photo and thermo- responsive polymers. The TEM image in **Figure 1c** shows a thin and uniform silica layer was coated on the hydrophobic nanoparticles by using the modified water-in-oil reverse microemulsion technique [26-27]. The thickness of silica shell is approximately 10 nm. The DLS results of OA-NaYF4: Yb/Tm core, UCNPs and UCNPs@$SiO_2$ are shown in **Figure S2**. Then the silica surface was modified with the coupling agent MPS to render the nanoparticles with carbon-carbon double bonds for further polymer coatings.

Since the azo groups are inhibited to the radical chain reaction by the azo group, it is difficult to form pure azo chromophores particles through emulsion [28]. Our group have successfully obtained photoresponsive polyazobenzene particles by using the distillation precipitation polymerization [22]. When the solvent is distilled at a constant rate, a high monomer conversion could be maintained and a lower monomer concentration at the start of the reaction can prevent the particles from aggregations [29]. In this work, distillation precipitation polymerization was adapted and modified to prepare DR-NCs, in which the UCNPs@$SiO_2$, thermal responsive NIPAM, and photoresponsive BMAAB were used as the template, monomer, and crosslinker, respectively. As shown in **Figure 1d**, monodisperse DR-NCs are obtained. We found that the dispersity of the resulting nanoparticles was influenced by the amount of solvent acetonitrile. A relatively large amount of acetonitrile was used to initiate the reaction of distillation precipitation polymerization, which made the particles not easy to adhere each other and improved the conversion rate of monomers. With solvent

acetonitrile (70 mL), crosslinking agent BMAAB (85 mg) and thermosensitive monomer NIPAM (213 mg), well dispersed DR-NCs were successfully synthesized. The effect of changing the monomer concentration and crosslinker amount on the thickness of shell were shown in **Figure S3**.

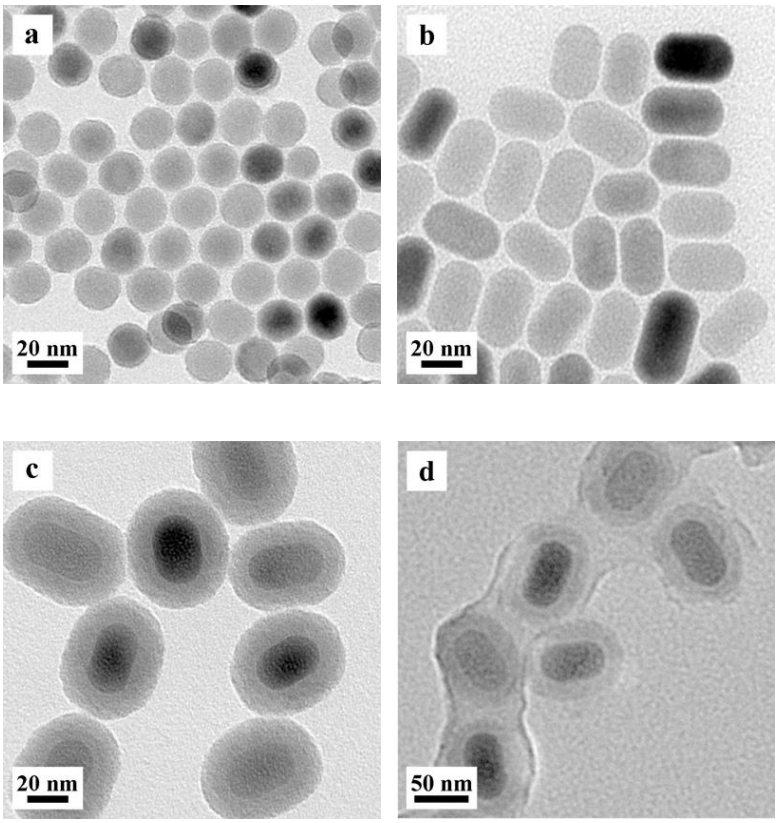


**Figure 1.** TEM images of (a) $NaYF_4$: $Yb^{3+}/Tm^{3+}$, (b) UCNPs, (c) UCNPs@$SiO_2$, (d) DR-NCs

*a) DXR Loading into DR-NCs*

DXR, a commonly used chemotherapeutic drug for cancer therapy, was selected as a model drug to evaluate the loading behaviors of the DR-NCs. DXR (positively charged) can strongly attach to DR-NCs surface (zeta potential: -40.6 mV) through hydrogen bonds and electrostatic interactions with the silanol groups, yielding DXR-DR-NCs [30]. A DXR loading ratio of 41 wt.% was measured by studying the absorbance at 480 nm of DXR solution before and after the loading

process. The loading performance is higher than other reported drug-loading up-conversion nanoparticle based systems [31-33]. Fluorescence micrographs of (a) DXR-DR-NCs, (b) after the release of DRX for 24 h under visible light, and (c) the solution outside the dialysis tube are shown in **Figure S4**.

*b) Thermal-responsive behavior of the DR-NCs*

As shown in **Figure S5**, the water contact angle of DR-NCs increased from 78.07° to 130.18° when the temperature increased from 25 °C to 47 °C. The transformation from hydrophilic to hydrophobic leaded to the shrinkage of DR-NCs at 47 °C. The PNIPAM molecules consisted of the hydrophilic amide groups and hydrophobic isopropyl groups, which could lead to the structural transformation according to temperature difference.

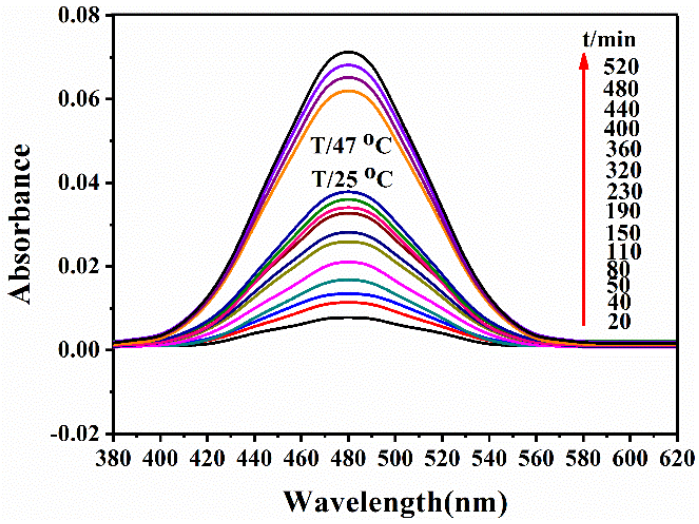


**Figure. 2** UV-vis spectra of DXR release from DR-NCs at 25 °C and 47 °C

After loading the DXR into DR-NCs, the thermal-controlled drug release behavior of DR-NCs was evaluated by measuring the UV-vis absorption spectra. **Figure 2** shows the UV-vis absorption spectrum of DXR released from DR-NCs at 25 °C and after it reached equilibrium, which shows a further release at 47 °C. As time increased, the absorbance of the DXR released from DR-NCs

at 480 nm also increased and reached the equilibrium after 360 minutes. Interestingly, when the temperature further increased to 47 °C, the absorbance of the DXR released from DR-NCs at 480 nm further increased and reached the equilibrium after 160 minutes. At 25 °C, ~27% of DXR was released after 360 min. However, ~51% of DXR was released after 160 min when temperature increased to 47 °C. When the temperature was higher than LCST, the surface of DR-NCs became hydrophobic and the shell shrunk and thus further increased the release rate. There are many works about the temperature-controlled release of nanoparticles. Similar findings were also reported that entrapped drug molecules can be squeezed out by changing the hydrophilicity of PNIPAM moiety [33-35].

*c) Photo-controlled release behavior of DXR-DR-NCs*

In the present work, azobenzene was used as a cross-linker because of its excellent reversible photo-isomerization behaviors. When the *trans* structure changes to *cis* structure, the distance between 4 and 4` carbons and its corresponding dipole moment are 9.0 Å and 0 D for the *tran*-isomer and 5.5 Å and 3 D for the *cis*-isomer, respectively [36]. As the crosslinker in the PNIPAM layer, the transformation of azobenzene structure would produce photomechanical effects to the entire system under the photoisomerization behaviors. The photoresponsive behavior of DR-NCs has been demonstrated in **Figure S6**. Polymer films of poly(ethyl acrylate) networks using main chain azo chromophores as cross-linker were first prepared by Eisenbach in 1980 [37]. Baczkowski M. L fabricated azobenzene-functionalized polyimides and showed large deformation due to photomechanical effects of azobenzene [38]. Our group incorporated the photomechanical effects into nanacapsules and successfully realized UV responsive controlled release [22]. In this work, we further improved the stability and functionality of UCNPs by adding an NIR-responsive feature and fine-tuning the synthetic process.

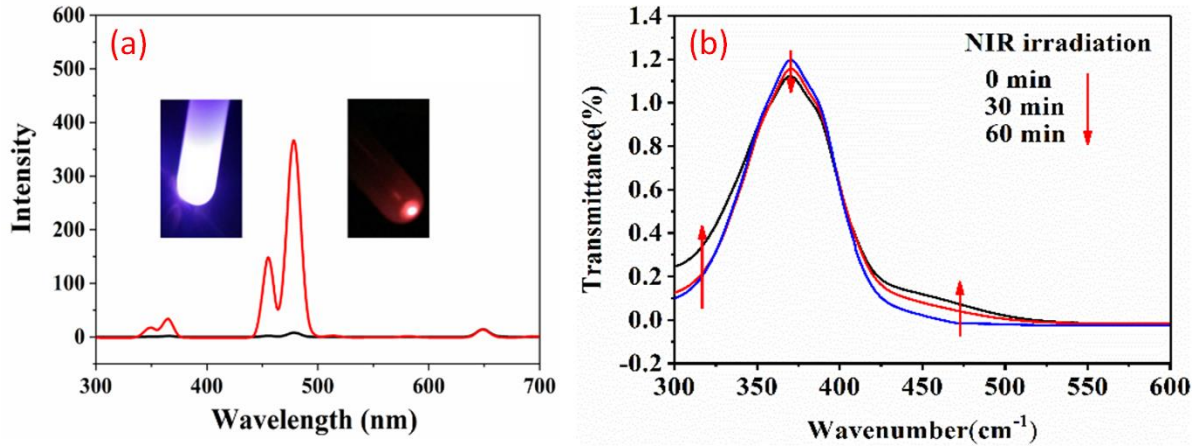


**Figure. 3** (a) Upconversion luminescent spectra of UCNPs (red) and DR-NCs (black), (b) UV-vis spectra of DR-NCs under 980 nm NIR irradiation at room temperature

Because of the unique optical properties, the upconversion luminescence of rare-earth nanoparticles has been extensively studied. Interestingly, autofluorescence and photodamage can be minimized with increased tissue penetration depth under 980 nm NIR irradiation. When excited at 980 nm, UCNPs have three emission wavelengths in the UV to visible range, which are from 365 nm from the $^1D_2$ state to the ground state $^3H_6$ emission. UV photons, $^1D_2$ to 450 nm from the intermediate $^3F_4$ and 475 nm visible blue photons radiated from $^1G_4$ to the ground state $^3H_6$. **Figure 3a** is the upconversion luminescent spectra of UCNPs (red) and DR-NCs (black). As shown in **Figure 3a**, the photoresponsive azobenzene at the crosslinking absorbed UV light emitted by the upconverting nanoparticles under excitation of NIR light. Compared to the luminescent spectra of UCNPs, DR-NCs had no luminescence spectrum at 365 nm. It can be fully proved that azobenzene absorbed UV and visible light (450 nm) emitted by UCNPs under NIR excitation. Both UCNPs and DR-NCs had luminescence spectra at 650 nm before and after azobenzene coating. The UV spectrum induced the *trans-cis* isomerization and reached at the equilibrium state after 60 minutes at 980 nm irradiation from **Figure 3b**. Under the simultaneous UV and visible light transmitted by

the UCNPs, the transmittance shift was not obvious, which indicated that the azobenzene movement reached a dynamic equilibrium. There are many works to investigate the isomerization behaviors of azobenzene under the simultaneous UV and visible light illumination. Fujiwara reported that azobenzene-modified mesoporous silica remarkably promote the release of molecules from the inside of the mesopore to the outside, when the lights, both UV and visible lights, were irradiated simultaneously [39]. Zink also reported similar results about the mesostructured silica particles in which the azobenzene acted as molecular machine to promote the release [40]. Shi prepared NIR-triggered drug delivery by upconverting nanoparticles with integrated azobenzene-modified mesoporous silica. The reversible photoisomerization by simultaneous UV and visible light emitted by the UCNPs creates a continuous rotation-inversion movement and act as a molecular impeller that propels the release of DXR [19]. In our work, the azobenzene at the dynamic equilibrium would also be in a continuous isomerization movement which would also act as a molecular machine to promote the release of the encapsulated molecules.

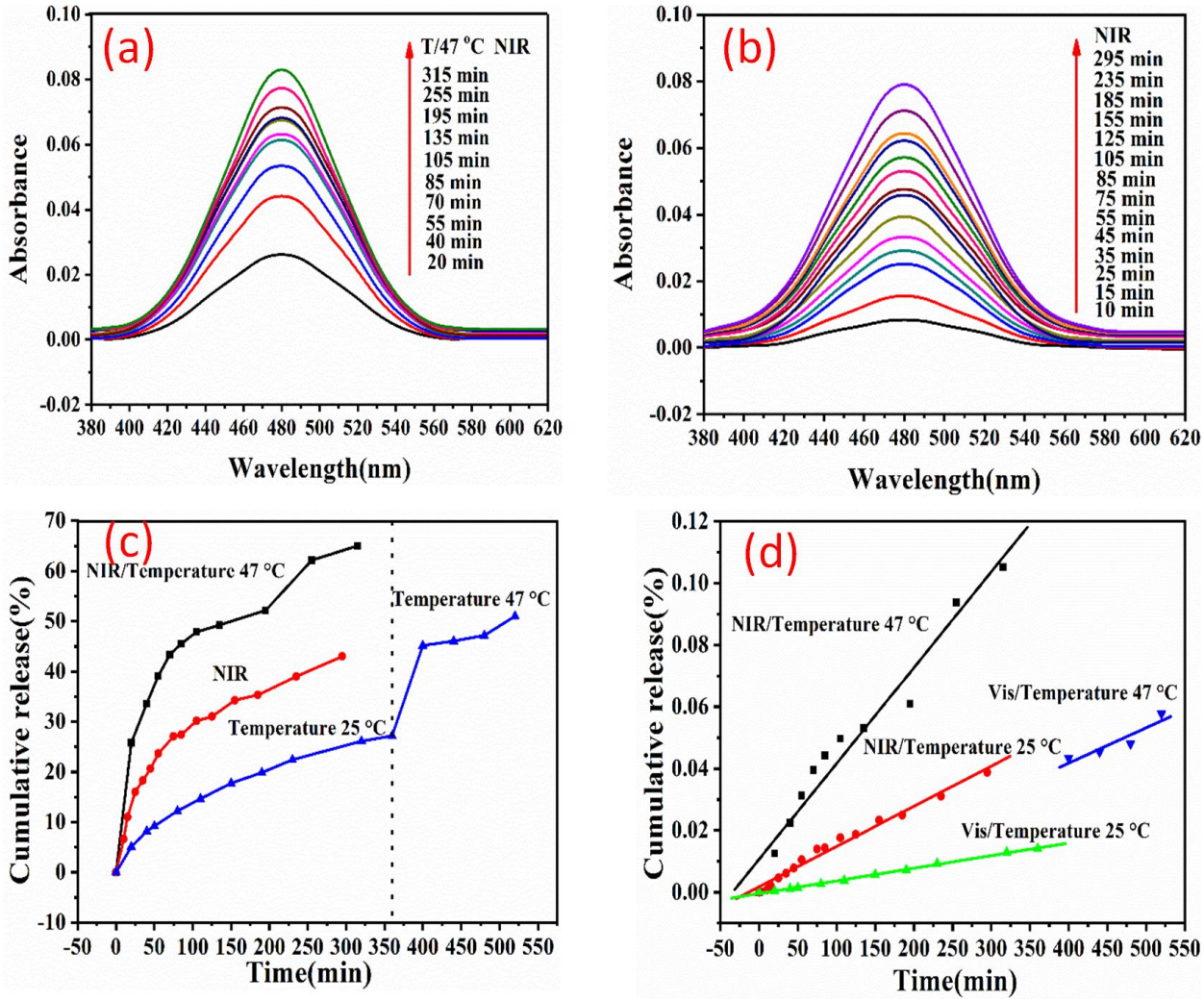


**Figure. 4**. UV-vis spectra of DXR release from DR-NCs (a) under NIR; (b) under NIR at 47 °C; and (c) Cumulative release of DXR from DR-NCs as a function of time under different conditions. (d) Linear regression analysis using the Baker-Lonsdale model profile.

The NIR-responsive release behavior of DXR-DR-NCs was also investigated. **Figure 4a** and **Figure 4b** show the UV-vis absorption spectrum of DXR released from DXR-DR-NCs under pure NIR light at 25 °C and 47 °C, respectively. Obviously, as time increased, the absorbance of the DXR released from DR-NCs at 480 nm also increased and reached an equilibrium after 295 minutes and 315 minutes, respectively. **Figure 4c** shows release profile of DXR from the

nanoparticles. Under NIR light, ~43% of DXR was released after 295 min. However, ~65% of DXR was released after 315 min when temperature increased to 47 °C and under NIR irradiation. The NIR was transformed to UV and visible light by the UCNPs, which caused the continuous movement of BMAAB and acted as a molecular machine to promote the release of DXR. Interestingly, when the temperature was increased higher than the LCST, the DR-NCs become hydrophobic, which leads to shrinkage of the nanoparticles. Therefore, the release of the DXR is faster under the NIR and at 47 °C.

Various models have been used to describe the release of drugs from different matrices. Among them, the Baker-Lonsdale model, appropriate for spherical system, could be applied for modeling the release of different conditions [41-43].

$$\frac{3}{2}\left[1-\left(1-\frac{M_t}{M_\infty}\right)^{\frac{2}{3}}\right]-\frac{M_t}{M_\infty}=\frac{3DC_s}{r_0^2C_0}\cdot t \qquad (1)$$

where $M_t$ and $M_\infty$ are the amounts of the DXR at time t and at infinite time, respectively; $M_t/M_\infty$ is the cumulative release percent of DXR; ***D*** is the diffusion coefficient of the molecules from the system; $r_0$ is the radius of the nanoparticles; $C_s$ is the solubility of the DXR in the system; and $C_0$ is the original concentration of DXR. The results in **Figure 4d** indicate that the Baker-Lonsdale model fitted well with the release profile of DXR under different conditions. The release rate constants ($3DC_s/r_0^2C_0$) and the correlation coefficients $R^2$ are $4.09\times10^{-5}$ and 0.99 (T = 25 °C, visible light), $1.14\times10^{-4}$ and 0.99 (T = 47 °C, visible light), $1.3\times10^{-4}$ and 0.99 (T = 25 °C, NIR light) and $3.1\times10^{-4}$ and 0.98 (T = 47 °C, NIR light), respectively. As in the same system, $C_s$ and $C_0$ are the same, the diffusion coefficient ***D*** under NIR irradiation is 31.8 times higher than the one irradiated with visible light at the same temperature 25 °C, demonstrating the release driven by photo-mechanical effect under NIR light. In addition, when temperature increased from 25 °C to

47 °C under visible light illumination, larger ***D*** (2.79 fold) was also obtained. The combination of higher temperature and NIR light led to larger release rate and amounts. About 65% of DXR released from the nanoparticles after 315 minutes. These results demonstrated that the endogenic temperature and ectogenic NIR illumination could be used to control the release of DXR. As the UCNPs can be further modified with photothermal materials (e.g. graphene oxide) [44], we have demonstrated a powerful nanoformulation for triggering the drug release remotely and tailoring its release profile by controlling illumination time and intensity.

## 4. Conclusions

In conclusion, a thermal and photo dual-responsive drug delivery system has been successfully synthesized based on a modified distillation precipitation polymerization method. The incorporation of UCNPs into a thermal-responsive polymer, PNIPAM, crosslinked by a photo-responsive crosslinker, BMAAB, produces the dual-responsive feature. BMAAB exhibits reversible photo-isomerization which can be triggered by the UV and visible light generated form the upconversion process of UCNPs. The shell movement induced by the transformation of azobenzene moieties acted as a molecular machine to facilitate the release of DXR under a NIR irradiation. In addition, the change of hydrophilicity of PNIPAM due to the increase of temperature furthered promoted the release of DXR, leading to ~65% of DXR release from the nanocarriers at 315 min (at 47 °C and NIR irradiation). Baker−Lonsdale model was used to determine the diffusion coefficients under different conditions. Our work reported the fabrication of UCNPs-PNIPAM core-shell polymeric drug nanocarriers, which exhibit dual responsive, good stability and high loading capacity. This opens up a great opportunity for designing smart drug nanocarriers for combating cancer.

## Acknowledgements

This work was financially supported by the Natural National Science Foundation of China (51303049, 51603065 and 31871442) and the Research Committee of The Hong Kong Polytechnic University (G-UABM).

## Supporting Information Available

Supporting Information includes: (i) FTIR and hydrodynamic diameters measurement of UCNPs, UCNPs@$SiO_2$ and DR-NCs; (ii) Fluorescence microscopy images of (a) DXR-DR-NCs at the beginning (t = 0) and (b) 24 hours after the release (t = 24 h) and (c) the solution outside the dialysis tubes; (iii) Water contact angles of DR-NCs at different temperatures; and (iv) UV-vis spectra of DR-NCs under different conditions.

## References

1. Biswas, Y.; Dule, M.; Mandal, T. K., Poly(Ionic Liquid)-Promoted Solvent-Borne Efficient Exfoliation of Mos2/Mose2 Nanosheets for Dual-Responsive Dispersion and Polymer Nanocomposites. *J. Phys. Chem. C* **2017**, *121*, 4747-4759.

2. Chen, C. K.; Wang, Q.; Jones, C. H.; Yu, Y.; Zhang, H. G.; Law, W. C.; Lai, C. K.; Zeng, Q. H.; Prasad, P. N.; Pfeifer, B. A.; Cheng, C., Synthesis of Ph-Responsive Chitosan Nanocapsules for the Controlled Delivery of Doxorubicin. *Langmuir* **2014**, *30*, 4111-4119.

3. Zhou, X.; Chen, L.; Nie, W.; Wang, W.; Qin, M.; Mo, X.; Wang, H.; He, C., Dual-Responsive Mesoporous Silica Nanoparticles Mediated Codelivery of Doxorubicin and Bcl-2 Sirna for Targeted Treatment of Breast Cancer. *J. Phys. Chem. C* **2016**, *120*, 22375-22387.

4. Karimi, M.; Zangabad, P. S.; Baghaee-Ravari, S.; Ghazadeh, M.; Mirshekari, H.; Hamblin, M. R., Smart Nanostructures for Cargo Delivery: Uncaging and Activating by Light. *J. Am. Chem. Soc.* **2017**, *139*, 4584-4610.

5. Chen, C.-K.; Law, W.-C.; Aalinkeel, R.; Yu, Y.; Nair, B.; Wu, J.; Mahajan, S.; Reynolds, J. L.; Li, Y.; Lai, C. K.; Tzanakakis, E. S.; Schwartz, S. A.; Prasad, P. N.; Cheng, C., Biodegradable

Cationic Polymeric Nanocapsules for Overcoming Multidrug Resistance and Enabling Drug–Gene Co-Delivery to Cancer Cells. *Nanoscale* **2014**, *6*, 1567-1572.

6. Mahajan, S. D.; Roy, I.; Xu, G.; Yong, K.-T.; Ding, H.; Aalinkeel, R.; Reynolds, J.; Sykes, D.; Nair, B. B.; Lin, E. Y.; Prasad, P. N.; Schwartz, S. A., Enhancing the Delivery of Anti Retroviral Drug "Saquinavir" across the Blood Brain Barrier Using Nanoparticles. *Curr. HIV Res.* **2010**, *8*, 396-404.

7. Chen, J.; Li, X.; Zhao, X.; Wu, Q.; Zhu, H.; Mao, Z.; Gao, C., Doxorubicin-Conjugated Ph-Responsive Gold Nanorods for Combined Photothermal Therapy and Chemotherapy of Cancer. *Bioactive Materials* **2018**, *3*, 347-354.

8. Chan, M.-H.; Chen, S.-P.; Chen, C.-W.; Chan, Y.-C.; Lin, R. J.; Tsai, D. P.; Hsiao, M.; Chung, R.-J.; Chen, X.; Liu, R.-S., Single 808 Nm Laser Treatment Comprising Photothermal and Photodynamic Therapies by Using Gold Nanorods Hybrid Upconversion Particles. *J. Phys. Chem. C* **2018**, *122*, 2402-2412.

9. Law, W. C.; Mahajan, S. D.; Kopwitthaya, A.; Reynolds, J. L.; Liu, M. X.; Liu, X.; Chen, G. Y.; Erogbogbo, F.; Vathy, L.; Aalinkeel, R.; Schwartz, S. A.; Yong, K. T.; Prasad, P. N., Gene Silencing of Human Neuronal Cells for Drug Addiction Therapy Using Anisotropic Nanocrystals. *Theranostics* **2012**, *2*, 695-704.

10. Mart, R. J.; Allemann, R. K., Azobenzene Photocontrol of Peptides and Proteins. *Chem. Commun.* **2016**, *52*, 12262-12277.

11. Weis, P.; Wu, S., Light-Switchable Azobenzene-Containing Macromolecules: From Uv to near Infrared. *Macromol. Rapid Comm.* **2018**, *39*.

12. Logtenberg, H.; Browne, W. R., Electrochemistry of Dithienylethenes and Their Application in Electropolymer Modified Photo- and Redox Switchable Surfaces. *Org. Biomol. Chem.* **2013**, *11*, 233-243.

13. Irie, M.; Fulcaminato, T.; Matsuda, K.; Kobatake, S., Photochromism of Diarylethene Molecules and Crystals: Memories, Switches, and Actuators. *Chem. Rev.* **2014**, *114*, 12174-12277.

14. Ma, L.; Li, J. Z.; Han, D.; Geng, H. P.; Chen, G. X.; Li, Q. F., Synthesis of Photoresponsive Spiropyran-Based Hybrid Polymers and Controllable Light-Triggered Self-Assembly Study in Toluene. *Macromol. Chem. Phys.* **2013**, *214*, 716-725.

15. Karthik, S.; Puvvada, N.; Kumar, B. N. P.; Rajput, S.; Pathak, A.; Mandal, M.; Singh, N. D. P., Photoresponsive Coumarin-Tethered Multifunctional Magnetic Nanoparticles for Release of Anticancer Drug. *ACS Appl. Mater. Interfaces* **2013**, *5*, 5232-5238.

16. Linsley, C. S.; Wu, B. M., Recent Advances in Light-Responsive on-Demand Drug-Delivery Systems. *Ther. Delivery* **2017**, *8*, 89-107.

17. Yan, B.; Boyer, J. C.; Branda, N. R.; Zhao, Y., Near-Infrared Light-Triggered Dissociation of Block Copolymer Micelles Using Upconverting Nanoparticles. *J. Am. Chem. Soc.* **2011**, *133*, 19714-19717.

18. Chen, S.; Gao, Y. J.; Cao, Z. Q.; Wu, B.; Wang, L.; Wang, H.; Dang, Z. M.; Wang, G. J., Nanocomposites of Spiropyran-Functionalized Polymers and Upconversion Nanoparticles for Controlled Release Stimulated by near-Infrared Light and Ph. *Macromolecules* **2016**, *49*, 7490-7496.

19. Liu, J. A.; Bu, W. B.; Pan, L. M.; Shi, J. L., Nir-Triggered Anticancer Drug Delivery by Upconverting Nanoparticles with Integrated Azobenzene-Modified Mesoporous Silica. *Angew. Chem., Int. Ed.* **2013**, *52*, 4375-4379.

20. Zhao, Y., Light-Responsive Block Copolymer Micelles. *Macromolecules* **2012**, *45*, 3647-3657.

21. Yan, K.; Chen, M.; Zhou, S. X.; Wu, L. M., Self-Assembly of Upconversion Nanoclusters with an Amphiphilic Copolymer for near-Infrared- and Temperature-Triggered Drug Release. *RSC Adv.* **2016**, *6*, 85293-85302.

22. Wang, X. T.; Huang, T.; Law, W. C.; Cheng, C. H.; Tang, C. Y.; Chen, L.; Gong, X. H.; Liu, Z. F.; Long, S. J., Controlled Encapsulation and Release of Substances Based on Temperature and Photoresponsive Nanocapsules. *J. Phys. Chem. C* **2018**, *122*, 3039-3046.

23. Wang, X. T.; Yang, Y. K.; Yang, Z. F.; Liao, Y. G.; Zhang, W.; Xie, X. L., Synthesis and Photo-Responsive Behaviors of Hollow Polyazobenzene Micro-Spheres. *Chin. Sci. Bull.* **2010**, *55*, 3441-3447.

24. Wang, X. T.; Yang, Y. K.; Liao, Y. G.; Yang, Z. F.; Jiang, M.; Xie, X. L., Robust Polyazobenzene Microcapsules with Photoresponsive Pore Channels and Tunable Release Profiles. *Eur. Polym. J.* **2012**, *48*, 41-48.

25. Wang, X. T.; Li, Z. H.; Yang, Y. K.; Gong, X. H.; Liao, Y. G.; Xie, X. L., Photomechanically Controlled Encapsulation and Release from Ph-Responsive and Photoresponsive Microcapsules. *Langmuir* **2015**, *31*, 5456-5463.

26. Law, W.-C.; Yong, K.-T.; Roy, I.; Xu, G.; Ding, H.; Bergey, E. J.; Zeng, H.; Prasad, P. N., Optically and Magnetically Doped Organically Modified Silica Nanoparticles as Efficient Magnetically Guided Biomarkers for Two-Photon Imaging of Live Cancer Cells. *J. Phys. Chem. C* **2008**, *112*, 7972-7977.

27. Yi, D. K.; Selvan, S. T.; Lee, S. S.; Papaefthymiou, G. C.; Kundaliya, D.; Ying, J. Y., Silica-Coated Nanocomposites of Magnetic Nanoparticles and Quantum Dots. *J. Am. Chem. Soc.* **2005**, *127*, 4990-4991.

28. Li, Y. B.; Deng, Y. H.; Tong, X. L.; Wang, X. G., Formation of Photoresponsive Uniform Colloidal Spheres from an Amphiphilic Azobenzene-Containing Random Copolymer. *Macromolecules* **2006**, *39*, 1108-1115.

29. Li, G. L.; Lei, C. L.; Wang, C. H.; Neoh, K. G.; Kang, E. T.; Yang, X. L., Narrowly Dispersed Double-Walled Concentric Hollow Polymeric Microspheres with Independent Ph and Temperature Sensitivity. *Macromolecules* **2008**, *41*, 9487-9490.

30. Knezevic, N. Z.; Trewyn, B. G.; Lin, V. S. Y., Light- and Ph-Responsive Release of Doxorubicin from a Mesoporous Silica-Based Nanocarrier. *Chem. - Eur. J.* **2011**, *17*, 3338-3342.

31. Tian, G.; Gu, Z. J.; Zhou, L. J.; Yin, W. Y.; Liu, X. X.; Yan, L.; Jin, S.; Ren, W. L.; Xing, G. M.; Li, S. J.; Zhao, Y. L., Mn2+ Dopant-Controlled Synthesis of Nayf4:Yb/Er Upconversion Nanoparticles for in Vivo Imaging and Drug Delivery. *Adv. Mater.* **2012**, *24*, 1226-1231.

32. Wang, C.; Cheng, L. A.; Liu, Z. A., Drug Delivery with Upconversion Nanoparticles for Multi-Functional Targeted Cancer Cell Imaging and Therapy. *Biomaterials* **2011**, *32*, 1110-1120.

33. Shankar, B. V.; Patnaik, A., A New Ph and Thermo-Responsive Chiral Hydrogel for Stimulated Release. *J. Phys. Chem. B* **2007**, *111*, 9294-9300.

34. Leal, M. P.; Torti, A.; Riedinger, A.; La Fleur, R.; Petti, D.; Cingolani, R.; Bertacco, R.; Pellegrino, T., Controlled Release of Doxorubicin Loaded within Magnetic Thermo-Responsive Nanocarriers under Magnetic and Thermal Actuation in a Microfluidic Channel. *ACS Nano* **2012**, *6*, 10535-10545.

35. Cui, W.; Lu, X. M.; Cui, K.; Niu, L.; Wei, Y.; Lu, Q. H., Dual-Responsive Controlled Drug Delivery Based on Ionically Assembled Nanoparticles. *Langmuir* **2012**, *28*, 9413-9420.

36. Finkelmann, H.; Nishikawa, E.; Pereira, G. G.; Warner, M., A New Opto-Mechanical Effect in Solids. *Phys. Rev. Lett.* **2001**, *87*.

37. Eisenbach, C. D., Isomerization of Aromatic Azo Chromophores in Poly(Ethyl Acrylate) Networks and Photomechanical Effect. *Polymer* **1980**, *21*, 1175-1179.

38. Baczkowski, M. L.; Wang, D. H.; Lee, D. H.; Lee, K. M.; Smith, M. L.; White, T. J.; Tan, L. S., Photomechanical Deformation of Azobenzene-Functionalized Polyimides Synthesized with Bulky Substituents. *ACS Macro Lett.* **2017**, *6*, 1432-1437.

39. Fujiwara, M.; Akiyama, M.; Hata, M.; Shiokawa, K.; Nomura, R., Photoinduced Acceleration of the Effluent Rate of Developing Solvents in Azobenzene-Tethered Silica Gel. *ACS Nano* **2008**, *2*, 1671-1681.

40. Angelos, S.; Johansson, E.; Stoddart, J. F.; Zink, J. I., Meslostructured Silica Supports for Functional Materials and Molecular Machines. *Adv. Funct. Mater.* **2007**, *17*, 2261-2271.

41. Kim, J. O.; Kabanov, A. V.; Bronich, T. K., Polymer Micelles with Cross-Linked Polyanion Core for Delivery of a Cationic Drug Doxorubicin. *J. Controlled Release* **2009**, *138*, 197-204.

42. Higuchi, T., Mechanism of Sustained-Action Medication. Theoretical Analysis of Rate of Release of Solid Drugs Dispersed in Solid Matrices. *J. Pharm. Sci.* **1963**, *52*, 1145-1149.

43. Hu, H. R.; Wang, H. T.; Du, Q. G., Preparation of Ph-Sensitive Polyacrylic Acid Hollow Microspheres and Their Release Properties. *Soft Matter* **2012**, *8*, 6816-6822.

44. Li, P.; Yan, Y.; Chen, B.; Zhang, P.; Wang, S.; Zhou, J.; Fan, H.; Wang, Y.; Huang, X., Lanthanide-Doped Upconversion Nanoparticles Complexed with Nano-Oxide Graphene Used for Upconversion Fluorescence Imaging and Photothermal Therapy. *Biomater. Sci.* **2018**, *6*, 877-884.

**TOC**

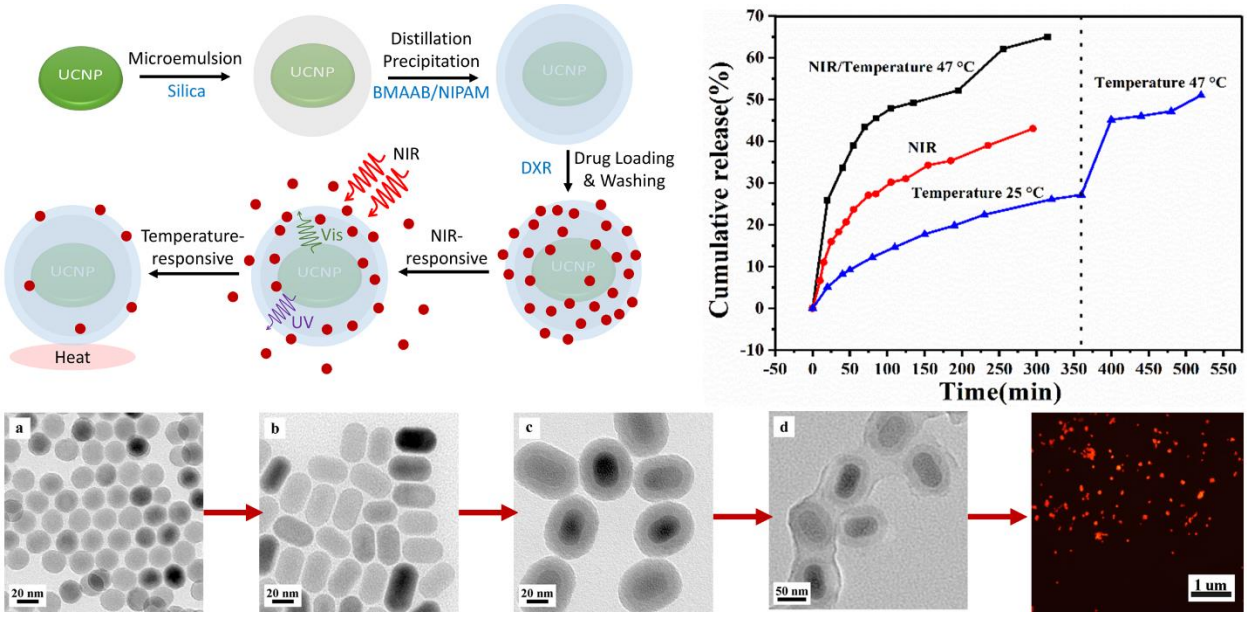
UCNP
Microemulsion
Silica
UCNP
Distillation
Precipitation
BMAAB/NIPAM
UCNP
DXR
Drug Loading
& Washing
NIR
Vis
UV
Temperature-
responsive
NIR-
responsive
UCNP
Heat
Cumulative release(%)
Time(min)
NIR/Temperature 47 °C
NIR
Temperature 25 °C
Temperature 47 °C
a
b
c
d
20 nm
20 nm
20 nm
50 nm
1 um